UNIVERSITY *of York*

This is a repository copy of *Analog B(M1) strengths in the Tz=± 32 mirror nuclei Mn 47 and Ti 47*.

White Rose Research Online URL for this paper:
https://eprints.whiterose.ac.uk/id/eprint/213483/

Version: Published Version

Article:

White Rose
university consortium
Universities of Leeds, Sheffield & York

eprints@whiterose.ac.uk
https://eprints.whiterose.ac.uk/

Analog $B(M1)$ strengths in the $T_z = \pm\frac{3}{2}$ mirror nuclei ^{47}Mn and ^{47}Ti

S. Uthayakumaar,[1,2] M. A. Bentley [ORCID],[1] R. Yajzey [ORCID],[3] D. Bazin [ORCID],[2,4] J. Belarge,[2] P. C. Bender,[2] P. J. Davies [ORCID],[1] B. Elman,[2,4]
A. Gade [ORCID],[2,4] T. Haylett,[1] H. Iwasaki [ORCID],[2,4] D. Kahl,[5,6] N. Kobayashi,[2] B. Longfellow,[2,4] S. J. Lonsdale,[5] E. Lunderberg,[2,4]
L. Morris,[1] D. R. Napoli [ORCID],[7] X. Pereira-Lopez [ORCID],[8,9] F. Recchia,[2,10] E. C. Simpson,[11] R. Wadsworth [ORCID],[1] and D. Weisshaar [ORCID][2]

[1]*School of Physics, Engineering and Technology, University of York, Heslington, York YO10 5DD, United Kingdom*
[2]*Facility for Rare Isotope Beams, Michigan State University, East Lansing, Michigan 48824, USA*
[3]*Physics Division, Department of Physical Sciences, College of Science, Jazan University, P.O. Box. 114, Jazan 45142, Saudi Arabia*
[4]*Department of Physics and Astronomy, Michigan State University, East Lansing, Michigan 48824, USA*
[5]*School of Physics and Astronomy, University of Edinburgh, Edinburgh EH9 3FD, United Kingdom*
[6]*Extreme Light Infrastructure – Nuclear Physics, Horia Hulubei National Institute for R&D in Physics*
and Nuclear Engineering (IFIN-HH), 077125 Bucharest-Măgurele, Romania
[7]*INFN, Laboratori Nazionali di Legnaro, I-35020 Legnaro, Italy*
[8]*Department of Physics, University of York, Heslington, York YO10 5DD, United Kingdom*
[9]*Center for Exotic Nuclear Studies, Institute for Basic Science (IBS), Daejeon 34126, Republic of Korea*
[10]*Dipartimento di Fisica e Astronomia dell'Università and INFN, Sezione di Padova, I-35131 Padova, Italy*
[11]*Department of Nuclear Physics and Accelerator Applications, Research School of Physics,*
The Australian National University, Canberra ACT 2600, Australia

The lifetimes of the first excited $\frac{7}{2}^-$ states in the $T_z = \pm\frac{3}{2}$ mirror nuclei ^{47}Mn and ^{47}Ti have been extracted utilizing the γ-ray line shape method, giving $\tau = 687(36)$ ps and $\tau = 331(15)$ ps respectively. Since these transitions are essentially pure $M1$ transitions, these results allow for a high-precision comparison of analog $M1$ strengths in mirror nuclei. The two analog $B(M1)$s are observed to be identical to a precision of about 10%. The expected dependence of the transition matrix element with T_z has been used to extract the separate isoscalar and isovector components of the transition strength, and the results are discussed in the context of predictions, based on the isospin formalism, regarding analog $B(M1)$ strengths.

I. INTRODUCTION

The neutron-proton exchange symmetry, rooted in the approximate charge symmetry and charge independence of the nucleon-nucleon interaction, is one of the most fundamental tenets in nuclear physics. The isospin concept [1] provided the framework to describe the resulting symmetries that are observed to occur in nuclei, i.e. isobaric analog states (IAS) of the same isospin quantum number T in an isobaric multiplet. The formalism of isospin provides the mathematical tools to allow the quantum-mechanical prediction of properties of those IAS, in a multiplet, as a function of T_z [$= (N - Z)/2$].

Predictions that follow from this formalism include the isobaric multiplet mass equation (see, e.g., [2] for a recent review), which describes energy splitting between IAS as a function of T_z and the various isospin rules that describe the T_z dependence of electromagnetic transition strengths between

pairs of IAS within the multiplet; see the description later in this article. Testing the predictions of the isospin formalism through measuring the T_z dependence of these properties is a crucial method of examining the isospin symmetry, and purity, of the states concerned. To date, precision tests of these predictions have had a strong focus on energy splitting across a multiplet, through precision measurements of masses (e.g., [2]) or excitation-energy differences through gamma-ray spectroscopy (e.g., [3–7]).

Testing the T_z dependence of electromagnetic transition strengths, however, presents significant experimental challenges, since it requires high statistics measurements of lifetimes in proton-rich systems. Nevertheless, such measurements can provide crucial insight into the underlying isospin symmetry of the wave functions, as well as providing information on the isospin-dependence of the electromagnetic transition operators through examination of the isoscalar and isovector components of the transition strength.

In the current work we present a high-precision measurement of the lifetimes of a pair of $T = \frac{3}{2}$ analog states in the $T_z = \pm\frac{3}{2}$ mirror nuclei ^{47}Mn / ^{47}Ti: the $J^\pi = \frac{7}{2}^-$ first-excited states. Since the transition in question is a virtually pure $M1$ transition, the analysis has enabled an unusually

precise comparison of analog $B(M1)$s in a mirror pair, and the first example of a high-precision comparison of such $B(M1)$ strengths in $T_z = \pm\frac{3}{2}$ mirrors. The T_z dependence of the $M1$ strength is analyzed and discussed.

II. EXPERIMENTAL PROCEDURE

The data presented in this work originate from an experiment that has been previously reported by Yajzey *et al.* [3] and Uthayakumaar *et al.* [4], where full details can be found of the experiment. The work presented here focuses solely on the lifetime measurements, and so the experimental details presented are limited to those specifically important for the lifetime analysis. The experiment was performed at the National Superconducting Cyclotron Laboratory (NSCL) at Michigan State University (MSU), using the A1900 separator [8] and the S800 spectrograph setup [9]. The A1900 was used to select beams of ^{48}Mn (≈ 84 MeV/u) and ^{48}V (≈ 89 MeV/u), in two separate sets of A1900 magnet settings, following fragmentation of a ^{58}Ni primary beam on a ^{9}Be target. These secondary beams impinged on a 188-mg cm^{-2} ^{9}Be reaction target. The nuclei of interest, ^{47}Mn and ^{47}Ti, were produced via one-neutron and one-proton knockout respectively, and these final fragments were identified, uniquely, through the standard time-of-flight and energy-loss methods [9], which are described in detail for this experiment in [3,4].

These two reactions are "analog" reactions: the two secondary beam species, ^{48}Mn and ^{48}V, are $T = 1$ mirror nuclei, and the "mirrored" reactions ($-1n$ and $-1p$ respectively) were used to populate analog states in the $T = \frac{3}{2}$ mirror nuclei ^{47}Mn and ^{47}Ti.

The prompt γ rays emitted in the reaction at the secondary target were detected using the Gamma-Ray Tracking In-beam Nuclear Array (GRETINA) [10,11]. For this measurement, GRETINA consisted of nine detector modules in two rings: four that were centered at 58° with respect to the beam axis, and five at 90° [3,4,10]. In this analysis, the first interaction in the GRETINA array was assumed to be that with the largest energy deposited, and the position of this interaction, determined from pulse-shape analysis, was used for the Doppler correction. Due to the very low energy ($\approx$120–160 keV) of the γ rays being analyzed here, GRETINA was analyzed in "single-crystal" mode, i.e., there were no add-back or tracking procedures employed that involve neighboring detectors. Indeed, for this γ-ray energy, it was observed that using the add-back procedure described in Ref. [4] reduces the photopeak efficiency compared with single-crystal mode.

III. RESULTS

A. Decay of the first excited state of $T_z = -\frac{3}{2}$ ^{47}Mn

A new level scheme of the proton-rich nucleus ^{47}Mn was recently established by Uthayakumaar *et al.* [4] from the same experiment, and reaction channel, as that being presented here. By far the strongest transition observed in ^{47}Mn in this experiment was a γ ray of around 123 keV. Given the very long lifetime of the state from which this transition decays (see below), and the comparison with the mirror nucleus, ^{47}Ti, this is clearly the decay of the first excited state in ^{47}Mn.

The analog first-excited state in ^{47}Ti is the 159-keV $J^{\pi} = \frac{7}{2}^-$ state, which has a published lifetime of $\tau = 303(9)$ ps [12], and which decays directly to the $J^{\pi} = \frac{5}{2}^-$ ground state. The analysis presented in Ref. [4] yielded a new level scheme for ^{47}Mn, and showed that the other populated levels, all of which have decay paths that flow through this 123-keV state, include the newly identified $\frac{9}{2}^-_{1,2}$, $\frac{11}{2}^-_{1,2}$, $\frac{13}{2}^-_1$, and $\frac{15}{2}^-_1$ states. The precise γ-ray energy of the decay from the ^{47}Mn first-excited state, and the lifetime of the state, have been determined by the analysis presented in this current work.

The γ-ray spectra presented here were obtained by selecting the incoming (^{48}Mn and ^{48}V) and outgoing (^{47}Mn and ^{47}Ti) nuclei using the standard particle identification procedure using the A1900 and S800 detectors as described in Ref. [4]. The velocity vector of the final nucleus, required for Doppler corrections, was determined on an event-by-event basis using the S800 tracking detectors [9]. A value for the velocity of the final nucleus, $\beta = \frac{v}{c}$, is required to perform Doppler correction and is a key parameter for the lifetime measurement. The transit time across the 1-mm-thick ^{9}Be secondary target is ≈ 10 ps, hence the value of β at the point of decay, for the long-lived transition being studied here, is the β corresponding to decays downstream of the target. This post-target β was determined event-by-event using the S800 tracking, with an average value determined by the S800 magnet settings. This yielded $\beta = 0.377$ for ^{47}Mn and $\beta = 0.396$ for ^{47}Ti. These values are used in the analysis that follows.

A low-energy (<180 keV) portion of the spectra created, following the above steps, is shown in Fig. 1 for (a) ^{47}Ti and (b) ^{47}Mn. Figure 1(a) shows that the γ-ray peak for ^{47}Ti has a clear low-energy, asymmetrical tailing as a result of the long lifetime of the state. Inspection of the ^{47}Mn spectrum, Fig. 1(b), shows a similar tail. The tailing effect is typical, for these experimental conditions, of decays from long-lived states with lifetimes >100 ps, for which the causes are detailed in Refs. [13,14]. The current evaluation for ^{47}Ti [12] derives the lifetime of this state, $\tau = 303(9)$ ps, from the weighted average of the results of Refs. [15,16]. The long tail on the high statistics transition around 123 keV in ^{47}Mn allows for a high-precision analysis of the lifetime of the newly observed first-excited state in ^{47}Mn. The analysis was performed first on the ^{47}Ti 159-keV transition, to validate the technique used, given that the lifetime is known to a high precision.

B. Lifetime measurements for the analog $J^{\pi} = \frac{7}{2}^-$ states

To perform the lifetime measurements, the experimental γ-ray peak shape was compared with the results of a simulation [17,18] based on the GEANT4 package [19]. The simulation, which takes into account the specific GRETINA geometry for this experiment, accounts for lifetime effects for a given transition, and allows for the addition of feeding transitions from higher-lying states. In the present analysis, all the the observed feeding states in ^{47}Ti have short lifetimes (< 3 ps), and it is assumed that the lifetimes of the analog feeding states in ^{47}Mn have similarly short lifetimes. Since the lifetimes under investigation are of the order of several hundred ps,
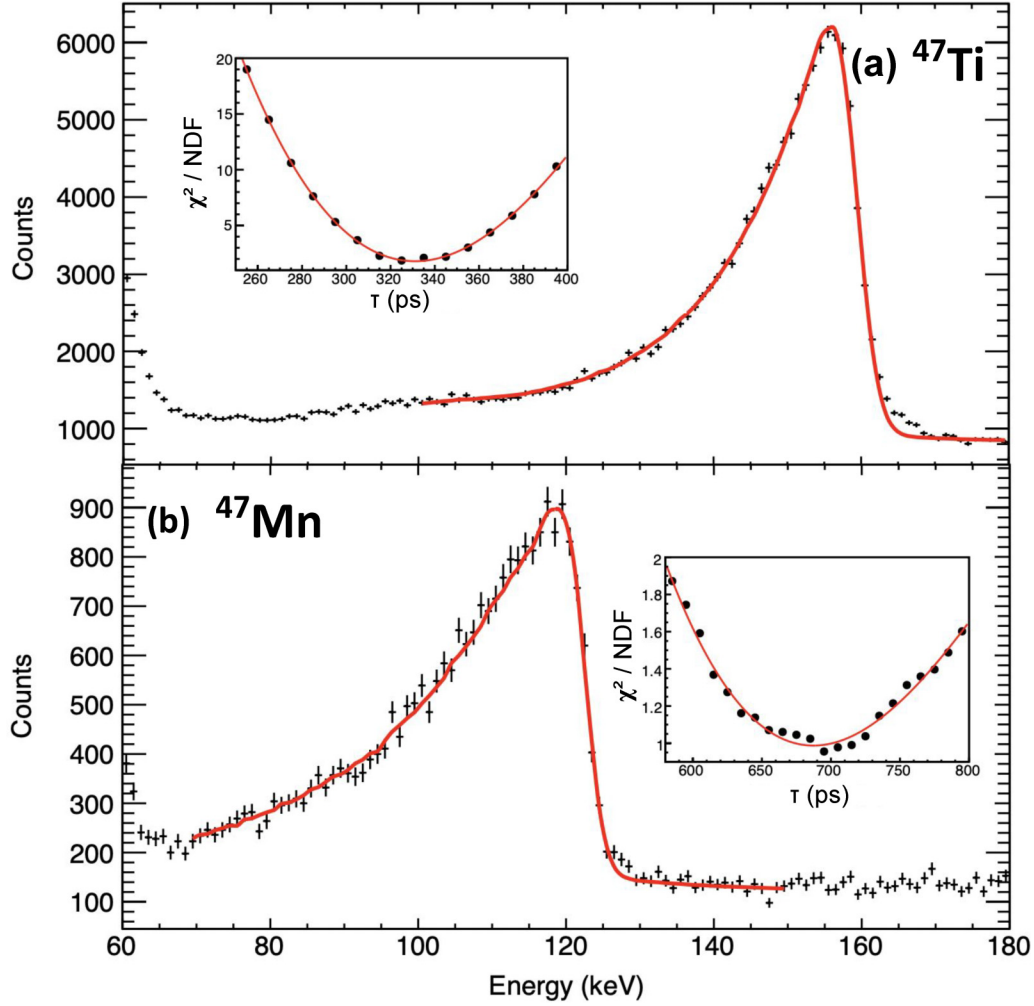
FIG. 1. The Doppler-corrected γ-ray spectra for (a) ^{47}Ti and (b) ^{47}Mn at velocities $\beta = 0.396$ and 0.377 respectively. The red line shows the simulated spectrum using the optimum best-fit parameters of $\tau = 331$ ps and $E_\gamma = 159.4$ keV for (a) and $\tau = 687$ ps and $E_\gamma = 122.6$ keV for (b). The inset plot presents the χ^2 per degree of freedom for a varying lifetime and using the optimum γ-ray energy obtained using the 2D χ^2-minimization procedure (see text for details).

it can be assumed that the addition of these states to the simulation would not have any significant impact on the extracted lifetime of the $\frac{7}{2}^-_1$ state. Hence, the decay of a single state alone was simulated. Setting up the simulation required specification of a number of reaction-related parameters, such as the secondary beam momentum spread and reaction-target-induced momentum spread, which were adjusted in order to reproduce the experimentally observed momentum spectrum. The effective position resolution for Doppler correction was also optimized to match experimental data. The two remaining key input parameters are the lifetime and the γ-ray energy. Both of these parameters were optimized for each peak; see below. In addition to the simulated spectrum, the background under the peak was simulated through the addition of a simple exponential background.

Simulations were then performed and fitted to the experimental peak shapes varying, systematically, the remaining two parameters: the γ-ray energy and the lifetime. A two-dimensional minimization procedure was followed to optimize both the γ-ray energy and the lifetime. The reasons for

allowing the γ-ray energy to vary are twofold. First, even if the γ-ray energy is known, there could be systematic effects in the experimental spectra (e.g., beam velocity or geometry) which could affect the apparent energy and hence bias the extracted lifetime. Second, the transition in ^{47}Mn is new to this work, and this procedure allows the γ-ray energy to be reliably determined. This two-dimensional (2D) χ^2-minimization procedure was demonstrated in Ref. [20] and recently employed in Ref. [13]. The results of the procedure are shown in Fig. 2 .

Once the global minimum χ^2 was found, from the data in Fig. 2(a), the optimum γ-ray energy was fixed, and the lifetime alone was varied to establish the χ^2/ndf plot, shown as the inset of Fig. 1(a). The minimum of this distribution was used to determine the optimum value of the lifetime.

Figure 1(a) shows the final fit for ^{47}Ti using the optimal parameters, found to be $\tau = 331$ ps and $E_\gamma = 159.4$ keV. For both ^{47}Ti and ^{47}Mn, a small high-energy tail, which cannot come from lifetime effects, was observed. This tail was also observed in Ref. [13]. One potential origin of this high-energy
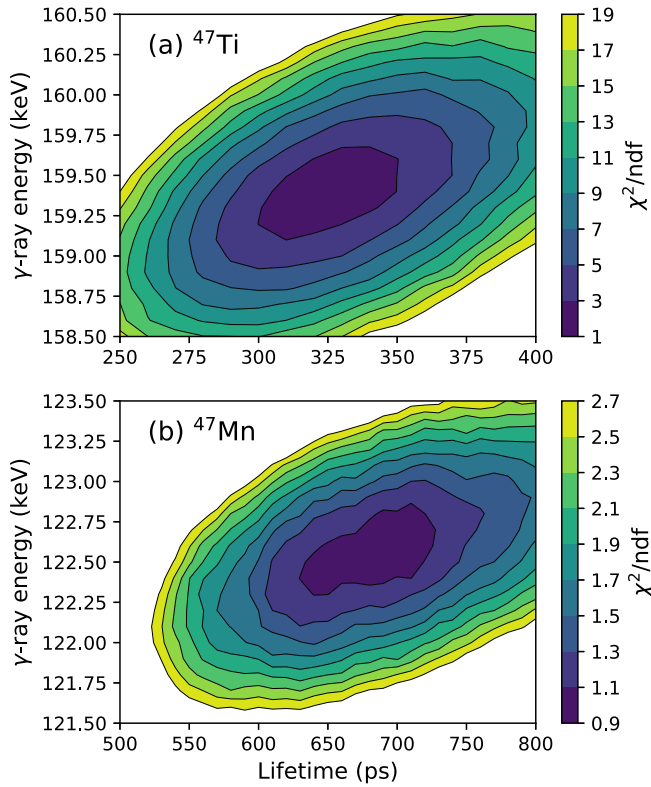
FIG. 2. Plots of χ^2 per degree of freedom having fitted the simulation to the spectra for (a) ^{47}Ti and (b) ^{47}Mn. The χ^2/ndf is plotted as a function of the lifetime and the γ-ray energy of the peak in question; see text for details.

tail may be due to the incorrect determination of the first interaction point in GRETINA for a small number of events. As in [13], a six-channel region on the right edge of the peak was excluded from the fit for this reason. The effect of the inclusion, or not, of this range has little effect on the extracted lifetime, but was nevertheless included in the systematic error. The statistical error in the lifetime was obtained from the $\chi^2 + 1$ value from the distribution in the inset in Fig. 1(a), having first normalized the χ^2 such that χ^2/ndf would have a minimum value of 1.0. The resulting error is then adjusted upwards to account for the correlation between E_γ and τ evident in Fig. 2. This was achieved by assuming that the contour of $\chi^2 + 1$ in the two-dimensional χ^2 surface has the same geometrical shape as that of the contours visible in Fig. 2. This procedure yields a statistical error of ± 4 ps. The main contributions to the systematic errors that were considered in this analysis are as follows. Errors associated with geometrical uncertainties (3%) and γ-ray anisotropy effects (1.5%) were included (assumed to be the same as in Refs. [13,17], which employed the same technique). For ^{47}Ti the uncertainty in the effective gamma-ray interaction position was assumed to be ± 1 mm, yielding a 1.9% error, and uncertainties in the determination of β gives a 0.7% error. In addition, there appears to be a systematic deviation from the simulation a for ≈ 6 channels around 148 keV, possibly indicating the presence of an unknown contamination peak. As a result, the range 144–150 keV was excluded from the fit as well as

the six-channel region described above. This increases the lifetime by 5 ps, and was also included as an additional systematic error. The total systematic error is then 14 ps. By adding both the statistical and systematic errors in quadrature, this yields a lifetime of $\tau = 331 \pm 4$ (stat.) ± 14 (sys.) ps $[T_{\frac{1}{2}} = 229(10)$ ps] for the $\frac{7}{2}^-_1$ state.

Having determined the lifetime, this procedure was repeated, for this fixed lifetime, to determine the final value of the γ-ray energy and its associated error. This yields $E_\gamma = 159.4$ keV. The line-shape fitting procedure is very sensitive to the energy of the γ ray, yielding a small statistical error of 0.3 keV. We have assumed a 1 keV systematic error, as with Ref. [4], to account for uncertainties in Doppler correction and energy calibration. These final values, $\tau = 331(15)$ ps and $E_\gamma = 159(1)$ keV, are both in reasonable agreement with the literature values of $\tau = 303(9)$ ps and $E_\gamma = 159.37(1)$ keV [12]. This provides a helpful validation of the methods used.

The identical procedure was then carried out for ^{47}Mn [Figs. 1(b) and 2(b)], where optimal values of $\tau = 687$ ps and $E_\gamma = 122.6$ keV were established. The statistical error in the lifetime was determined to be ± 17 ps. The systematic errors in this case were geometrical uncertainties (3%), anistropy (1.5%), β uncertainty (1.3%), position resolution (2.3%), and exclusion of the high-energy tail (0.9%). Below ≈ 70 keV in both spectra, there is a large broad structure, presumably due to radiative electron capture (see the low-energy edge of the spectra in Fig. 1). This has the potential to disturb the results for ^{47}Mn, and so the effect of varying the lower end of the fit range was investigated and used to determine a further systematic error of 1.6%. The final systematic error is therefore 32 ps. This yields a final result of $\tau = 687 \pm 17$ (stat.) ± 32 (sys.) ps. The γ-ray energy had the same 0.3 keV statistical error as with the ^{47}Ti transition, and the same systematic error was applied, yielding $E_\gamma = 123(1)$ keV.

The 159-keV γ-ray transition from the $\frac{7}{2}^-_1$ state in ^{47}Ti is known to be a near-pure $M1$ transition with only a very small contribution from the $E2$ component [12]. Combining the current result of $\tau = 331(15)$ ps with the two previous values [15,16] yields a new weighted average of $\tau = 309(7)$ ps. The current evaluated $B(E2) \downarrow$ strength for the 159.4-keV transition, from Coulomb excitation data, is 243(43) e^2fm^4 [12] which, when combined with the new lifetime gives $B(M1) = 0.0445(10)\mu_N^2$ with $|\delta| = 0.098(9)$. This corresponds to the M1 component being $\approx 99\%$ of the total strength. The final values for the lifetimes and the $B(E2)$ and $B(M1)$ in ^{47}Ti are shown in Table I.

For the 123-keV transition in ^{47}Mn, we have no experimental information on the mixing ratio and hence the $B(M1)$ and $B(E2)$ strengths cannot be independently determined. However, following the approach used in Ref. [20], we can consider the combinations of values of the $B(M1)$ and $B(E2)$ for ^{47}Mn for a range of possible mixing ratios; see the solid line in Fig. 3. Immediately it can be seen that the the value of the unknown $B(E2)$, for the 123-keV transition in ^{47}Mn, has very little impact on the corresponding $B(M1)$ value, again due to the low γ-ray energy which forces the transition to be completely dominated by the $M1$ component. As an exercise, we have allowed the $B(E2)$ in ^{47}Mn to vary by a factor of 100
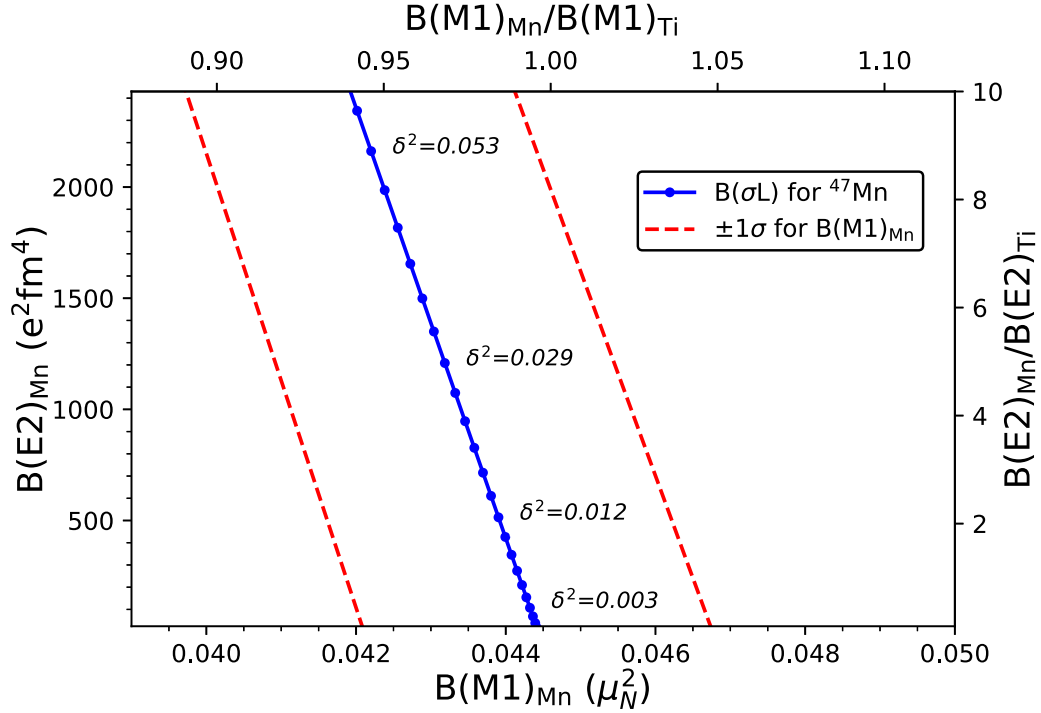
FIG. 3. Solid blue line and data points: Values along this line correspond, for the 123 keV transition in ^{47}Mn, to the $B(M1)$ (see principal x axis) and the corresponding $B(E2)$ (see principal y axis) consistent with the experimentally measured lifetime of the $\frac{7}{2}^{-}_{1}$ state in ^{47}Mn. The resulting ratio of the analog $B(M1)$ values for the $A = 47$ mirror pair (Mn/Ti) is plotted on the upper x axis and the ratio of the analog $B(E2)$ values on the right y axis. The data points correspond to values of $|\delta|$ of 0.03 to 0.24 in steps of 0.01. Red dashed lines: The limits ($\pm 1\sigma$) on $B(M1)$ for ^{47}Mn.

from 24.3 to 2430 e^2fm^4 ($\approx$2.4–240 W.u.). The lower end of the range is ten times smaller than the corresponding analog $B(E2)$ value in ^{47}Ti, and the upper value is ten times higher. This large range of $B(E2)$ values results in a variation of the ^{47}Mn $B(M1)$ from 0.044(2) to 0.042(2)μ_N^2. Since there is no known mechanism that could cause $B(E2)$ strengths in mirror

TABLE I. Comparison of the experimental and theoretical lifetimes and $B(M1)$ and $B(E2)$ transition strengths for decays from the $\frac{7}{2}^{-}_{1}$ state to the $\frac{5}{2}^{-}_{1}$ ground state in the ^{47}Ti and ^{47}Mn mirror pair. The mixing ratio for the transition in ^{47}Mn is unknown, therefore the $B(M1)$ and $B(E2)$ strengths have not been uniquely determined. The shell-model predictions used the effective charges from Dufour and Zuker [21] ($\epsilon_p = 1.31$, $\epsilon_n = 0.46$) and bare nucleon g factors. The experimental energies were used to obtain the shell-model lifetimes.

	^{47}Ti	^{47}Mn
Experiment		
Lifetime (ps)	309(7)[a]	687(36)
$B(M1)$ (μ_N^2)	0.0445(10)	
$B(E2)$ (e^2fm^4)	243(43)[b]	
Shell Model		
Lifetime (ps)	734	1486
$B(M1)$ (μ_N^2)	0.0187	0.0203
$B(E2)$ (e^2fm^4)	125	214

[a]Weighted average of the current result with those of Refs. [15,16].
[b]Current evaluation [12].

nuclei to differ by an order of magnitude, we consider that this range (the range displayed in Fig. 3) contains all physically reasonable combinations of $B(E2)$ and $B(M1)$ for ^{47}Mn. This is the range chosen for the data presented in Fig. 3 and used in the subsequent analysis.

While we cannot learn anything from these new results about the comparison of the analog $B(E2)$ strengths for decays from these analog $T_z = \pm \frac{3}{2}$, $J^\pi = \frac{7}{2}^{-}$ states, Fig. 3 shows that the ratio of the $B(M1)$ strengths between the mirrors remains well constrained, even with this conservatively chosen range of possibilities; see the top axis of Fig. 3. The red dashed lines in Fig. 3 contain the error bounds ($\pm 1\sigma$) for $B(M1)_{\text{Mn}}$. Considering the full range of possibilities between the dashed lines yields $B(M1)_{\text{Mn}} = 0.0432(35)\mu_N^2$. Taking into account the error in $B(M1)_{\text{Ti}}$, the ratio of the two $B(M1)$'s is then constrained to be $\frac{B(M1)_{\text{Mn}}}{B(M1)_{\text{Ti}}} = 0.97(8)$. That is, the two analog $J^\pi = \frac{7}{2}^{-} \rightarrow \frac{5}{2}^{-}$ transitions in the $T_z = \pm \frac{3}{2}$ mirrors have identical $M1$ strengths within a precision (1σ) of around 10%. Due to the high statistics of the measurement reported here, the comparison of the analog $B(M1)$ strengths has an unusually high precision, compared with typical lifetime measurements in very proton-rich systems. Moreover, the two $B(M1)$s have been determined in an identical (i.e. analog) reaction process and performed under identical experimental conditions. This gives a high confidence to the comparison. Hence, the resulting observation that the experimental $B(M1)$s are essentially identical is worthy of further discussion.

IV. DISCUSSION

Theoretical analysis of how transition matrix elements vary for analog states within a mutiplet has been presented in a number of texts, perhaps the most comprehensive being by Warburton and Wesener [22], where a number of isospin "rules" have been derived that describe the T_z dependence of electromagnetic transition matrix elements. The most general rule is that, in the limit of pure isospin (perfect isospin symmetry of the analog wavefunctions), the transition matrix elements for analog $T \to T$ transitions should be precisely linear in T_z. A recent analysis of this rule for $B(E2)$ transitions can be found in Ref. [23]. Testing the veracity of these rules is developing into a key approach to testing isospin purity in nuclei. In the case of analog transitions in a pair of mirror nuclei, the linearity rule cannot be tested and, apart from the specific case of $E1$ transitions, there is no exact rule that predicts, on the basis of isospin symmetry, the specific comparative behavior of "mirrored" transitions. In the case of $M1$ transitions, however, there is a "quasi" (approximate) rule [22], described later in this section.

The total transition matrix element, for an isospin-conserving $(T \to T)$ transition between states J_i and J_f, is determined by

$$M_{(\sigma L)} = \langle J_f M_f : T T_z | H_{(\sigma L)} | J_i M_i : T T_z \rangle; \qquad (1)$$

see Ref. [22] for a full description. Since the nuclear current density can be separated into an isoscalar and an isovector part, this allows an equivalent separation in the interaction:

$$H_{(\sigma L)} = H_{(\sigma L)}^{(0)} + H_{(\sigma L)}^{(1)}, \qquad (2)$$

where $H_{(\sigma L)}^{(0)}$ and $H_{(\sigma L)}^{(1)}$ represent the isoscalar and isovector interactions respectively. With this separation complete, the Wigner-Eckart thereom can be applied in isospin to extract the T_z dependence of the total transition matrix element; see [22] for details. Having further reduced the matrix elements in angular momentum, the reduced transition strength $B(\sigma L)$ can be written as

$$B(\sigma L) = \frac{1}{2J_i + 1} \left[M_{(\sigma L)}^{(0)} + \frac{T_z}{\sqrt{(2T+1)(T+1)T}} M_{(\sigma L)}^{(1)} \right]^2, \qquad (3)$$

where

$$M_{(\sigma L)}^{(0)} = \langle J_f \| H_{(\sigma L)}^{(0)} \| J_i \rangle,$$
$$M_{(\sigma L)}^{(1)} = \langle J_f : T \| | H_{(\sigma L)}^{(1)} \| | J_i : T \rangle.$$

The isoscalar part of Eq. (3) (the first term) contains no explicit isospin dependence. The isovector component of the transition [second term in Eq. (3)] depends on both T and T_z. $M_{(\sigma L)}^{(1)}$ has been reduced in isospin and both $M_{(\sigma L)}^{(0)}$ and $M_{(\sigma L)}^{(1)}$ have been reduced in angular momentum. Inserting the relevant values of T and T_z into Eq. (3) yields, for the current work,

$$B(M1)_{T = |T_z| = \frac{3}{2}} = \frac{1}{2J_i + 1} \left[M_{(M1)}^{(0)} \pm \sqrt{\frac{3}{20}} M_{(M1)}^{(1)} \right]^2, \qquad (4)$$

where $\pm$ corresponds to the sign of T_z. Equation (4) therefore shows that for a pair of mirrored ($T \to T$) transitions, for which T_z has opposite signs, identical $B(M1)$ strengths can only occur if either one of $M_{(M1)}^{(0)}$ or $M_{(M1)}^{(1)}$ is significantly smaller, in absolute magnitude, than the other.

Following the approach of Fujita *et al.* [24] it is possible to adapt Eq. (4) to define separate isoscalar and isovector $B(M1)$ strengths as follows:

$$B(M1)_{T = |T_z| = \frac{3}{2}}^{\text{IS}} = \frac{1}{2J_i + 1} \left[M_{(M1)}^{(0)} \right]^2,$$
$$B(M1)_{T = |T_z| = \frac{3}{2}}^{\text{IV}} = \frac{1}{2J_i + 1} \frac{3}{20} \left[M_{(M1)}^{(1)} \right]^2.$$

Fujita *et al.* [24] showed that these two components can be connected to the analog $B(M1)$s in a mirror pair. Solving Eq. (4) simultaneously yields

$$B(M1)^a = \tfrac{1}{4} [\sqrt{B(M1)_+} - \sqrt{B(M1)_-}]^2, \qquad (5)$$

$$B(M1)^b = \tfrac{1}{4} [\sqrt{B(M1)_+} + \sqrt{B(M1)_-}]^2, \qquad (6)$$

where $B(M1)_\pm$ corresponds to the analog transitions with $T_z = \pm T$. One of $B(M1)^a$ or $B(M1)^b$ corresponds to $B(M1)^{\text{IS}}$ and the other to $B(M1)^{\text{IV}}$. Since it is commonly assumed that magnetic dipole transitions are dominated by the isovector component, it could be assumed (as was done in other work, e.g., [24]) that the larger of these [i.e., $B(M1)_b$], is the isovector one. However, it is not possible, *a priori*, to specify which is which.

Considering all the data between the dashed ($\pm 1\sigma$) lines in Fig. 3 yields $B(M1)_- = 0.0432(35)\mu_N^2$, and combining this with the updated value of $B(M1)_+$ yields, for this analog pair of transitions

$$B(M1)^a = 2_{-2}^{+13} \times 10^{-6} \, \mu_N^2,$$
$$B(M1)^b = 4.38(18) \times 10^{-2} \, \mu_N^2.$$

From this analysis, it appears that one of the two components of the $B(M1)$ transition strengths is about four orders of magnitude smaller than the other. This observation can be made possible only by the high precision measurements of both $B(M1)$'s; see the form of Eq. (5). It should also be noted that while these separate components can be extracted from experimental data, doing so relies on the assumption of perfect isospin symmetry of the analog wave functions. While the vanishingly small component [i.e., $B(M1)_a$] is most likely the isoscalar component, this assignment cannot be explicitly made.

Fujita *et al.* [24] performed an extensive analysis of analog transition strengths in the $T_z = \pm \frac{1}{2}$ $A = 27$ mirror nuclei, through measurements of the mirrored $B(M1)$'s as well as analog $B(GT)$ values. They measured $B(M1)^{\text{IS}}$ and $B(M1)^{\text{IV}}$ for three excited states of the mirror pair. Generally they found that $B(M1)^{\text{IV}}$ was 1–2 orders of magnitude larger. In the current work, the lower limit for $B(M1)^b/B(M1)^a$, using the 3σ range for $B(M1)^a$ is >1000.

The values of $M_{(M1)}^{(k)}$ are determined by the application of the magnetic dipole operator, $\boldsymbol{\mu}$, which, again, has an isoscalar

and isovector part. This can be written (e.g., [24])

$$\boldsymbol{\mu} = \left[\sum_i^A \left(\frac{1}{2} g_s^{(0)} \boldsymbol{\sigma}_i + g_l^{(0)} \boldsymbol{l}_i \right) - \sum_i^A \boldsymbol{\tau}_z^{(i)} \left(\frac{1}{2} g_s^{(1)} \boldsymbol{\sigma}_i + g_l^{(1)} \boldsymbol{l}_i \right) \right] \mu_N, \tag{7}$$

where $g_{s(l)}^{(0)} = \frac{1}{2}(g_{s(l)}^{\pi} + g_{s(l)}^{\nu})$ are the isoscalar g factors and $g_{s(l)}^{(1)} = \frac{1}{2}(g_{s(l)}^{\pi} - g_{s(l)}^{\nu})$ are the isovector g factors. $\boldsymbol{\sigma}, \boldsymbol{l}$ are the usual spin and orbital angular momentum operators and $\boldsymbol{\tau}_z$ is the isospin projection operator, the eigenvalues of which are $+1$ for neutrons and -1 for protons. It is the first term in Eq. (7) which leads directly to $M_{(M1)}^{(0)}$ and the second term to $M_{(M1)}^{(1)}$. Examination of Eq. (7) reveals the origin of the usual dominance of the isovector term. The opposite signs of the proton and neutron spin g factors lead to $g_s^{(0)} = 0.88$ and $g_s^{(1)} = 4.71$, a factor of ≈ 5 difference. The orbital term $g_l^{(0)} \boldsymbol{l}_i$ can also partly cancel the spin term in the isoscalar matrix element (see [22]). Warburton and Wesener [22] estimated the relative magnitude of matrix elements for single-particle transitions of purely isoscalar and purely isovector nature (i.e., revised "Weisskopf-type" estimates). While such estimates are only approximate, it was found that the total transition matrix element for a purely isovector transition of single-particle strength was around an order of magnitude greater (absolute value) than that for a purely isoscalar transition. This would lead to ≈ 2 orders of magnitude difference in $B(M1)$. Thus, the expectation is that, for strong transitions (i.e., ≈ 1 W.u.), the isovector matrix element will be expected to dominate strongly.

The above argumentation led to the "quasi" rule that $M1$ transition strengths in mirror nuclei should be (quoting Ref. [22]) "of approximately equal strength within, say, a factor of two, if the transitions are of average strength or stronger." It is pointed out in Ref. [22] that the strong dominance of the isovector term is only guaranteed for strong transitions, i.e., of single-particle strength. In the current work, this is not the case: the transitions observed here are much weaker with $B(M1)^{\text{total}} \approx 0.03$ W.u. Thus, the theoretical conditions for the usual dominance of the isovector component may not be present here.

Skorka *et al.* [25] in 1966 performed an analysis of $\Delta T = 0$ and $|\Delta T| = 1$ $M1$ transitions in $A < 40$, $N = Z$ nuclei, the former being restricted (through isospin selection rules) to being purely isoscalar in nature and the latter to being purely isovector. It was found that the isoscalar $M1$ transitions ranged from ≈ 0.0001 to ≈ 0.1 W.u., with a quoted average of ≈ 0.005 W.u in Ref. [25], while isovector transitions ranged from ≈ 0.01 to ≈ 10 W.u., with a quoted average of ≈ 0.4 W.u. On the assumption that the larger measured component, $B(M1)_b$, is indeed the isovector one, the value extracted here would be at the bottom end of the observed range for isovector transitions. With that assignment, the $B(M1)^{\text{IS}}$ value from this work would be at least an order of magnitude below the bottom end of the typical range observed in Ref. [25]. We can provide no explanation for this, other than a coincidental numerical cancellation of different terms.

Shell-model calculations have been performed to predict the $B(M1)$ and $B(E2)$ for the analog transitions being studied

in this work. Calculations were performed using the ANTOINE code [26,27] using the KB3G interaction [28] in the full fp space. For determination of the $B(M1)$, bare-nucleon g factors were used while for the $B(E2)$ strengths the effective charges of Duflo and Zuker [21] ($\epsilon_p = 1.31$, $\epsilon_n = 0.46$) were used. The experimental energies were used in order to make a prediction of the lifetimes. As expected, the $B(E2)$ (and therefore the choice of effective charges) has virtually no impact on the predicted lifetime, since the strength is completely dominated by the $M1$ (predicted to be $\approx 99\%$ of the strength for both nuclei). The predicted $B(M1)$ strengths are small in magnitude and very similar in value, as in the experimental observations. Both are about a factor of 2 smaller than the experimental values, resulting in proportionally longer lifetimes. It is likely that cross-shell excitations between the sd and fp shells, which are missing in this shell-model interaction, would be required to improve the agreement. Despite the poor agreement between the experiment and theory on the magnitude of the $B(M1)$'s, the theoretical ratio of $B(M1)^{\text{IV}}/B(M1)^{\text{IS}}$ is ≈ 2400, consistent with the experimental value of $B(M1)^b/B(M1)^a$, when the 1σ error ranges are considered.

V. CONCLUSIONS

The lifetimes of the first-excited $J^\pi = \frac{7}{2}^-$ states in the $T_z = \pm\frac{3}{2}$ $A = 47$ mirror nuclei ^{47}Mn and ^{47}Ti have been measured using a Doppler-shift line-shape method. The lifetime for this state in ^{47}Mn, which has been observed for the first time in this experiment, was measured to be $\tau = 687(36)$ ps, compared with $\tau = 331(15)$ ps for its analog state in ^{47}Ti. The analysis has enabled a high-precision comparison of analog $M1$ strengths, with the two $B(M1)$'s being shown to be identical to within $\approx 10\%$. The formalism for the isospin-dependence of electromagnetic transition strengths has been applied to the experimental data to extract the isoscalar and isovector components of the reduced transition probability, $B(M1)$. One of these two components, most likely the isovector one, is found to completely dominate over the other by four orders of magnitude.

The processed experimental data generated during the current study are available in the University of York repository [29].

[1] E. Wigner, Phys. Rev. **51**, 106 (1937).
[2] M. MacCormick and G. Audi, Nucl. Phys. A **925**, 61 (2014).
[3] R. Yajzey *et al.*, Phys. Lett. B **823**, 136757 (2021).
[4] S. Uthayakumaar *et al.*, Phys. Rev. C **106**, 024327 (2022).
[5] A. Fernández *et al.*, Phys. Lett. B **823**, 136784 (2021).
[6] M. A. Bentley, S. M. Lenzi, S. A. Simpson, and C. A. Diget, Phys. Rev. C **92**, 024310 (2015).
[7] S. M. Lenzi, M. A. Bentley, R. Lau, and C. A. Diget, Phys. Rev. C **98**, 054322 (2018).
[8] D. J. Morrissey, B. M. Sherrill, M. Steiner, A. Stolz, and I. Wiedenhoever, Nucl. Instrum. Methods Phys. Res., Sect. B **204**, 90 (2003).
[9] D. Bazin, J. A. Caggiano, B. M. Sherrill, J. Yurkon, and A. Zeller, Nucl. Instrum. Methods Phys. Res., Sect. B **204**, 629 (2003).
[10] D. Weisshaar *et al.*, Nucl. Instrum. Methods Phys. Res., Sect. A **847**, 187 (2017).
[11] S. Paschalis *et al.*, Nucl. Instrum. Methods Phys. Res. Sect. A **709**, 44 (2013).
[12] T. W. Burrows, Nucl. Data Sheets **108**, 923 (2007).
[13] R. D. O. Llewellyn *et al.*, Phys. Rev. Lett. **124**, 152501 (2020).
[14] A. M. Hill, A. Gade, D. Bazin, B. A. Brown, B. Elman, P. Farris, J. Li, B. Longfellow, J. Pereira, A. Revel, D. Rhodes, M. Spieker, and D. Weisshaar, Phys. Rev. C **104**, 014305 (2021).
[15] M. Toulemonde, N. Schulz, J. C. Merdinger, and P. Engelstein, Phys. Rev. C **13**, 1889 (1976).
[16] D. C. S. White, W. J. McDonald, D. A. Hutcheon, and G. C. Neilson, Nucl. Phys. A **260**, 189 (1976).
[17] A. Lemasson, H. Iwasaki, C. Morse, D. Bazin, T. Baugher, J. S. Berryman, A. Dewald, C. Fransen, A. Gade, S. McDaniel, A. Nichols, A. Ratkiewicz, S. Stroberg, P. Voss, R. Wadsworth, D. Weisshaar, K. Wimmer, and R. Winkler, Phys. Rev. C **85**, 041303(R) (2012).
[18] P. Adrich, D. Enderich, D. Miller, V. Moeller, R. P. Norris, K. Starosta, C. Vaman, P. Voss, and A. Dewald, Nucl. Instrum. Methods Phys. Res. Sect. A **598**, 454 (2009).
[19] S. Agostinelli *et al.*, Nucl. Instrum. Methods Phys. Res. Sect. A **506**, 250 (2003).
[20] S. A. Milne *et al.*, Phys. Rev. C **93**, 024318 (2016).
[21] M. Dufour and A. P. Zuker, Phys. Rev. C **54**, 1641 (1996).
[22] E. K. Warburton and J. Weneser, in *Isospin in Nuclear Physics*, edited by D. H. Wilkinson (North-Holland, Amsterdam, 1969), Chap. 5.
[23] A. Boso *et al.*, Phys. Lett. B **797**, 134835 (2019).
[24] Y. Fujita, B. A. Brown, H. Ejiri, K. Katori, S. Mizutori, and H. Ueno, Phys. Rev. C **62**, 044314 (2000).
[25] S. J. Skorka, J. Hertel, and T. W. Retz-Schmidt, Nuclear Data Sheets. Sect. A **2**, 347 (1966).
[26] E. Caurier and F. Nowacki, Acta Phys. Pol. B. **30**, 705 (1999).
[27] E. Caurier, G. Martinez-Pinedo, F. Nowacki, A. Poves, and A. P. Zuker, Rev. Mod. Phys. **77**, 427 (2005).
[28] A. Poves, J. Sánchez-Solano, E. Caurier, and F. Nowacki, Nucl. Phys. A **694**, 157 (2001).
[29] M. Bentley, Open access data for the paper "Analogue B(M1) strengths in the Tz = ±3/2 mirror nuclei 47Mn and 47Ti", University of York (2022), 10.15124/6ac56aba-6665-426e-83e4-3ad3d384ca7c.